JoT JOURNAL OF TURBULENCE

http://jot.iop.org/

Determination of subfilter energy in large-eddy simulations

Johan Meyers and Martine Baelmans

Department of Mechanical Engineering, Katholieke Universiteit Leuven, Celestijnenlaan 300A, B3001 Leuven, Belgium
E-mail: Johan.Meyers@Mech.Kuleuven.ac.be

Received 6 May 2004
Published 9 August 2004
doi:10.1088/1468-5248/5/1/026

Abstract. A methodology is presented for the determination of the subfilter energy in large-eddy simulations (LES). The model assumes universal-equilibrium turbulence in the subgrid scales and is based on the integration of semi-empirical functions for energy spectra of homogeneous isotropic turbulence. The model depends on the Reynolds number, the integral length scale and its ratio to the flow containment, as well as the LES resolution. On the one hand, the formalism is suitable for an *a priori* estimation of the subgrid-energy level, which is useful for preparatory LES set-up. Charts are drawn which connect the Reynolds number and the LES resolution to the expected level of subgrid energy. Furthermore, the difference is evaluated between the present model and a model based on the integration of an idealized $k^{-5/3}$ spectrum, which is related to the high-Reynolds-number asymptotic behaviour of the energy spectrum. On the other hand, the presented methodology can be used as a model for the subgrid energy in an actual LES, as part of a subgrid-scale stress model. The formulation of the model, based on equations which directly use resolved-scale LES properties, is briefly outlined.

PACS numbers: 47.11.+j, 47.27.−i, 47.27.Eq, 47.27.Jv, 47.27.Gs

JoT 5 (2004) 026

 PII: S1468-5248(04)80293-8 1468-5248/04/000001+17$30.00

Contents

1. Introduction

Large eddy simulations (LES) are increasingly evolving as an important simulation technique for the prediction of turbulent flows. The advantage of this technique is its relative low computational cost, compared with the direct simulation of the Navier–Stokes equations, while—at least in potential—accurate results can be obtained. In LES, this is achieved by filtering the original Navier–Stokes equations. The aim of this filtering operation is to reduce the dynamic contents or number of modes in the solution of the *filtered* Navier–Stokes equations, such that they can be solved on a much coarser grid and, hence, at much lower cost than direct numerical simulation would require. Typically, the effects of the removed modes are then accounted for in an averaged way, using a subgrid-scale model. Furthermore, accuracy can be pursued by retaining the large and most relevant modes of the turbulent flow solution.

Throughout the years, a number of reviews, describing different techniques in LES in detail, have been presented (see e.g. [1]–[5]). There both accurate discretization methods and subgrid-scale models are identified as important issues in LES. Apart from modelling and discretization issues, which are of importance for the resolved LES scales, it is self-evident that part of the flow physics—corresponding to the subgrid scales—is not represented in the resolved LES solution. In an ideal situation, i.e. LES without modelling and discretization errors, these subgrid scales correspond to

$$\phi_{sgs}^{ideal} = \phi_{DNS} - \overline{\phi}_{DNS}, \qquad (1)$$

where $\overline{(\cdot)}$ is the filter operation, which corresponds to e.g. a sharp cut-off filter or grid truncation, and ϕ is a flow property of interest. To obtain an accurate representation of ϕ in the *resolved* LES scales, it is implicitly assumed that the effective number of modes in $\overline{\phi}_{DNS}$, which are ideally obtained from the *filtered* Navier–Stokes equations, are representative of the actual behaviour of ϕ_{DNS} itself. In fact, it is ϕ_{DNS}, which corresponds to the physical solution of the turbulent flow. Hence, the specific physical features one is interested in should be sufficiently retained in the reduced representation $\overline{\phi}_{DNS}$. For example, in this context, Geurts and Leonard [6] claim that the lack of modes in the filtered Navier–Stokes equations might, for a number of actual LES in the literature, be the main cause of erroneous results, rather than excessive errors in modelling or discretization. In fact, one often advises for good LES to choose the filter (or grid) cut-off, in the inertial subrange of turbulence, at an energy level which is at least one to two orders of magnitude lower than the energy level of the large-scale turbulence.

Nevertheless, corresponding to its main principles, LES only *resolves* large-scale turbulent phenomena. If *unresolved* scales are to be quantified, one basically resorts to three possible strategies, i.e. either refine the LES filter, perform DNS right away or, for statistical, ensemble-averaged quantities, formulate a model which accounts for the unresolved part of the statistics. The latter is mainly done for the unresolved turbulent kinetic energy, for which—in most cases as part of a subgrid-scale model—several examples are known [7]–[10]. For example, both the LES of the well-known Comte-Bellot [11] testcase is presented in [7, 8], where the LES initially resolves only 60–70% of the total turbulent kinetic energy. Both authors present models for the subgrid energy, which succeed in predicting the remaining 20–30% of the energy.

The methodologies presented to determine the subgrid energy fall into two categories, i.e. those which assume a turbulent equilibrium range [8, 12], leading to an algebraic expression for the subgrid energy, and those which solve a transport equation for the subgrid energy [7, 9, 10]. In the former category, Misra and Pullin [8] use a $k^{-5/3}$ spectrum to estimate the subgrid energy, which is further used in a vortex-based subgrid model.[1] Similarly, based on a $k^{-5/3}$ spectrum, Knaepen *et al* [12] use a dynamic formulation to shape a model for the subfilter energy. Related to the choice for a $-5/3$ spectrum, these models assume very high Reynolds numbers together with an LES filter which is situated in the inertial subrange.

The present paper concentrates on the determination of the subgrid energy based on an equilibrium assumption for the energy spectrum. By use of well-known semi-empirical descriptions of the energy spectrum of homogeneous isotropic turbulence [13], a model is presented which includes important parameters such as the Reynolds number, and the integral length scale and its ratio to the dimension of the flow containment. This formulation is not restricted to the high-Reynolds-number limit, and the LES-filter cut-off may be situated in the universal equilibrium range rather then only in the inertial subrange. Although this model is limited to cases where the subgrid scales are in the universal equilbrium range, it can—in contrast with the more sophisticated subgrid-energy transport models—be used to perform an *a priori* estimation of subgrid-energy levels. As a consequence, this formulation can serve different main goals.

(1) First of all it enables an *a priori* estimation of the subgrid-scale energy. This type of estimation can be used in a preparatory phase of a large-scale LES. Results are helpful for the choice of mesh size with respect to the fraction of energy represented in the resolved scales. As a further consequence, the presented analysis can indicate in which situations an explicit model for the subgrid energy is needed.

(2) Furthermore, the model can effectively be used in LES to provide the subgrid energy and can e.g. be plugged into any eddy-viscosity type subgrid-scale model, or in more complex formulations such as the one presented in [8]. Self-evidently, one should take care that the subgrid scales are effectively situated in a universal equilibrium range.

[1] In fact, the use of a simplified representation of the energy spectrum as a $-5/3$ spectrum is standard practice, e.g., Jiménez and Moser [14] use a $-5/3$ spectrum as an intermediate to estimate the correlation between subgrid-scale stress and strain in LES; and Lilly [15] uses it to determine the theoretical Smagorinsky constant.

(3) Finally, the estimation of the subgrid energy and its relative share of the total energy might be one of the parameters in an extensive error analysis of LES, as a too-large fraction of subgrid energy is potentially useful as an indicator for low quality of the resolved scale dynamics. In fact, the accurate representation of the kinetic energy in the resolved scales of the simulations is often conceived as an important indicator for the quality of LES.

The present paper mainly focuses on the first item on this list, supplemented with a brief comment on how the second item can effectively be realized. Reynolds number dependence is studied, and the limits for which the much simpler $k^{-5/3}$ spectrum provides accurate estimations are outlined. Results show that—with respect to the prediction of the subgrid energy—an idealized $-5/3$ spectrum can only be used for fairly high Reynolds numbers, i.e. $Re_\lambda > 1000$. Although main emphasis is on the subgrid energy, extension towards other properties is simple, as long as they can be expressed in terms of the energy spectrum, i.e. quantities that are quadratic in the velocity.

Although the proposed methodology is based on properties of homogeneous isotropic turbulence, it is assumed that these results can also be used for free shear flows in general, provided they display locally isotropic small-scale turbulence. This conjecture will be further supported in this paper by the fact that results are shown to be almost independent of the low-wavenumber, large-scale resolution of the spectrum. In addition, as first pointed out by Lumley [16], for weak shear, anisotropic stresses typically decay with $k^{-4/3}$ compared with $k^{-2/3}$ for the isotropic stresses.

The paper is further organized as follows. First, in section 2, a short overview is presented on the analytical expressions used to describe the energy spectrum of homogeneous isotropic turbulence. Next, in section 3, the relative subgrid energy is determined. Based on the analytical expressions for the energy spectrum, this subgrid energy is evaluated as a function of Reynolds number and filter-width and the expected asymptotic behaviour is studied. Furthermore, the effective quality of this *a priori* estimation is validated using DNS of decaying homogeneous isotropic turbulence at two different Reynolds numbers. The formulation of the subfilter-energy model, such that it can be directly used in LES, is also briefly outlined. Finally, conclusions are presented in section 4.

2. Energy spectra for homogeneous isotropic turbulence

In the present section, a short overview is presented on the properties of energy spectra of homogeneous isotropic turbulence. In this context, a set of core relations is presented at which analytical proposals for energy spectra should comply. The theoretical relations presented in this section are a concise review of ideas presented in some standard textbooks, such as by Hinze [13], Monin and Yaglom [17] and Pope [18], supplemented with some slight elaborations, needed in the scope of the present paper.

First, in section 2.1, the analytical expressions used in the present paper are introduced. Next, in section 2.2, a set of relations at which these analytical expressions should comply is introduced and the sensitivity of the expressions with respect to relevant physical parameters is elaborated. Finally, in section 2.3, the formulations presented in sections 2.1 and 2.2 are extended towards finite-domain systems with periodic boundary conditions.

2.1. Energy spectra

At present, it is generally accepted that all high-Reynolds-number flows exhibit some universal features in the small turbulent scales, i.e. the inertial subrange and the dissipation range of turbulence. Kolmogorov [19]–[21] presented a major theory on this universal scaling (K41). As a result of this theory, the universal formulation of the energy spectrum in the universal subrange and beyond can be written as

$$E(k) = \alpha \varepsilon^{2/3} k^{-5/3} f_\eta(k\eta) \quad \text{for } k \gg 1. \tag{2}$$

In this equation, $\eta = (\nu^3/\varepsilon)^{1/4}$ is the Kolmogorov scale. Also, $f_\eta(k\eta)$ is a damping function, which adapts the $-5/3$th behaviour of the inertial subrange towards a steeper fall of energy in the dissipation range of the spectrum. Hence, f_η has a value of 1 in the inertial subrange and has a universal shape in the dissipation region. At present, no exact analytical expression is known for $f_\eta(k\eta)$. Several expressions, based on simplified theories and empirical observations, such as e.g. the Heisenberg and Pao spectra, were presented in the past (see e.g. [13, 17] for an overview).

On the low-wavenumber side of the turbulent spectrum, no universal behaviour exists and observations vary strongly depending on the flow type, the Reynolds number, etc. Nevertheless, for homogeneous isotropic turbulence, the low wavenumber behaviour of the spectrum is well known [17, 18] and corresponds to experimental observations. This results in a 'low-wavenumber damping function' $f_L(kL)$. It adapts the $-5/3$th law at the low end of the spectrum and has a value of 1 at the inertial subrange and beyond. Furthermore, L is an integral length scale of the same order of magnitude as the energy containing eddies. It is defined by

$$L = \frac{E^{3/2}}{\varepsilon}. \tag{3}$$

Pope [13] successfully presents an expression for f_η and f_L which will be further used in this paper, i.e.

$$E(k) = \alpha \varepsilon^{2/3} k^{-5/3} f_L(kL) f_\eta(k\eta), \tag{4}$$

with

$$f_L(kL) = \left(\frac{kL}{[(kL)^2 + c_L]^{1/2}} \right)^{11/3} \tag{5}$$

and

$$f_\eta(k\eta) = \exp(-\beta([(k\eta)^4 + c_\eta^4]^{1/4} - c_\eta)). \tag{6}$$

As previously deemed necessary, these functions clearly satisfy

$$\lim_{k\to 0} f_L(kL) = 0, \qquad \lim_{k\to\infty} f_L(kL) = 1$$

and

$$\lim_{k\to 0} f_\eta(k\eta) = 1, \qquad \lim_{k\to\infty} f_\eta(k\eta) = 0. \tag{7}$$

Equations (4)–(6) are unequivocally fixed, provided the total energy level E, the integral length scale L and the Reynolds number Re_λ are set. In fact, ε can be determined from L and E using (3). Taking into account the definition of $\eta = (\nu^3/\varepsilon)^{1/4}$, one obtains

$$Re_L \equiv \frac{E^{1/2} L}{\nu} = \left(\frac{L}{\eta} \right)^{4/3}. \tag{8}$$

With the transversal Taylor Reynolds number

$$\lambda = \left[\frac{4}{3}E \Big/ \left\langle\left(\frac{\partial u_1}{\partial x_2}\right)^2\right\rangle\right]^{1/2}, \tag{9}$$

and $Re_\lambda = u'\lambda/\nu$, it can be further elaborated that [13]

$$Re_L = \tfrac{3}{20}Re_\lambda^2. \tag{10}$$

Since (8) expresses a relationship between L, η and the Reynolds number Re_L, it is possible to define 'full range' damping functions, i.e.

$$f(k\eta) = f_L(k\eta Re_L^{3/4})f_\eta(k\eta) \tag{11}$$

and

$$F(kL) = f_L(kL)f_\eta(kLRe_L^{-3/4}), \tag{12}$$

where $f(k\eta) = F(kL)$.

In (5) and (6), three parameters, i.e. c_L, c_η and β, remain undetermined. These parameters can be calculated based on a set of prerequisites at which appropriate descriptions of the energy spectrum should comply. This will be presented in the next subsection.

2.2. Consistency relations for damping functions

In this subsection, we will focus on the determination of c_L, c_η and β, which consists of a slight generalization of the methodology presented by Pope [13]. This results in an infinite set of consistency relations at which any analytical expression for an energy spectrum should comply. Naturally—as long as the 'exact' description of the universal damping function is not found—it is only feasible to satisfy a restricted set of these equations. In case of the analytical formulation used in this paper (cf (4)–(6)) only the first three consistency relations comply.

First, a non-dimensional formulation of the energy spectrum is considered, i.e.

$$g(k\eta) = (k\eta)^{-5/3}f(k\eta) = \frac{E(k)}{\alpha\varepsilon^{2/3}\eta^{5/3}}. \tag{13}$$

By expressing the zeroth, second and fourth moments of the non-dimensional energy spectrum $g(k\eta)$, three relations are easily obtained which can be used to determine c_L, c_η and β:

$$\mathcal{M}_0 \equiv \int_0^\infty g(k\eta)\,\mathrm{d}(k\eta) = \frac{\int_0^\infty E(k)\,\mathrm{d}k}{\alpha\nu^{1/2}\varepsilon^{1/2}} = \frac{Re_L^{1/2}}{\alpha}, \tag{14}$$

$$\mathcal{M}_2 \equiv \int_0^\infty (k\eta)^2 g(k\eta)\,\mathrm{d}(k\eta) = \frac{\eta^{4/3}\int_0^\infty 2\nu k^2 E(k)\,\mathrm{d}k}{2\alpha\varepsilon^{2/3}\nu} = \frac{1}{2\alpha} \tag{15}$$

and

$$\mathcal{M}_4 \equiv \int_0^\infty (k\eta)^4 g(k\eta)\,\mathrm{d}(k\eta) = \frac{\eta^{10/3}\int_0^\infty k^4 E(k)\,\mathrm{d}k}{\alpha\varepsilon^{2/3}} = \frac{\nu\langle S_{ij}\nabla^2 S_{ij}\rangle}{2\sqrt{2}\alpha\langle S_{ij}S_{ij}\rangle^{3/2}}. \tag{16}$$

The non-dimensional forms (14)–(16) express the demand that the corresponding energy spectrum, enstrophy spectrum and the palinstrophy spectrum integrate to the full energy E, enstrophy $\mathscr{E} = \frac{1}{2}\langle\omega_i\omega_i\rangle$ and palinstrophy $\mathcal{P} = \frac{1}{2}\langle(\nabla\times\boldsymbol{\omega})^2\rangle$, respectively.

Furthermore, (14) and (15) directly relate to standard physical flow properties such as the Reynolds number and the Kolmogorov constant. With some extra assumptions and relations for homogeneous isotropic turbulence, this is also achieved for (16). To this end, consider the enstrophy equation [22]

$$\frac{\mathrm{d}\frac{1}{2}\langle\omega_i\omega_i\rangle}{\mathrm{d}t} = \langle\omega_i\omega_j S_{ij}\rangle - 2\nu\langle S_{ij}\nabla^2 S_{ij}\rangle, \tag{17}$$

where ω_i is the ith component of the vorticity vector $\boldsymbol{\omega} = \nabla\times\boldsymbol{u}$. For high-Reynolds-number flows, local equilibrium for the enstrophy $\langle\omega_i\omega_i\rangle/2$ can be assumed, i.e. the left-hand side of (17) can be neglected in comparison with the terms on the right-hand side. Thus $\langle\omega_i\omega_j S_{ij}\rangle \approx 2\nu\langle S_{ij}\nabla^2 S_{ij}\rangle$. This can be combined with the following standard isotropy relations [17]:

$$\langle S_{ij}S_{ij}\rangle = \frac{15}{2}\left\langle\left(\frac{\partial u_1}{\partial x_1}\right)^2\right\rangle \tag{18}$$

and

$$\langle\omega_i\omega_j S_{ij}\rangle = -\frac{35}{2}\left\langle\left(\frac{\partial u_1}{\partial x_1}\right)^3\right\rangle. \tag{19}$$

Eventually, this leads to

$$\mathcal{M}_4 = \frac{\langle\omega_i\omega_j S_{ij}\rangle}{4\sqrt{2}\alpha\langle S_{ij}S_{ij}\rangle^{3/2}} = \frac{-7}{12\sqrt{15}\alpha}\frac{\langle(\partial u_1/\partial x_1)^3\rangle}{\langle(\partial u_1/\partial x_1)^2\rangle^{3/2}} = \frac{-7\mathcal{S}_3}{12\sqrt{15}\alpha}, \tag{20}$$

where $\mathcal{S}_3$ is the skewness of the longitudinal velocity derivative. This property is often determined in experiments and DNS and is linked to the dissipation range behaviour of turbulence. It is generally accepted that at high Reynolds numbers, $\mathcal{S}_3$ is almost independent of the Reynolds number. Values of $-\mathcal{S}_3$ in experiments and DNS typically range from 0.3 to 0.9.

Since $f(k\eta)$ and consequently $\mathcal{M}_0 - \mathcal{M}_4$ depend on c_L, c_η, β and Re_L, (14), (15) and (20) lead to a nonlinear system of equations

$$\begin{bmatrix}\mathcal{M}_0(c_L, c_\eta, \beta, Re_L)\\ \mathcal{M}_2(c_L, c_\eta, \beta, Re_L)\\ \mathcal{M}_4(c_L, c_\eta, \beta, Re_L)\end{bmatrix} = \frac{1}{\alpha}\begin{bmatrix}Re_L^{1/2}\\ 1/2\\ \frac{-7}{12\sqrt{15}}\mathcal{S}_3\end{bmatrix}. \tag{21}$$

This system of equations can be seen as the first three consistency relations for damping functions. It is clear that an infinite set of equations could be considered, which would couple the shape of the damping function, i.e. its moments, to a full range of physical higher-order ensemble-averaged quantities.

Equation (21) can be solved numerically using simple numerical techniques such as e.g. Gauss quadrature, etc. In figure 1 the sensitivity of c_L, c_η and β to Re_λ and $\mathcal{S}_3$ is addressed. First, in figure 1(a), $\mathcal{S}_3$ is fixed at -0.7 and the dependency of the coefficients on Re_λ is plotted. Clearly, all coefficients have a finite asymptote for $Re_\lambda \to \infty$, with $c_{L,\infty} = 6.783$, $c_{\eta,\infty} = 0.402$ and $\beta_\infty = 5.3$. Figure 1(b) displays the relative change of the coefficients, i.e. by normalizing them with their asymptotic values. Clearly, c_η and β are nearly independent of

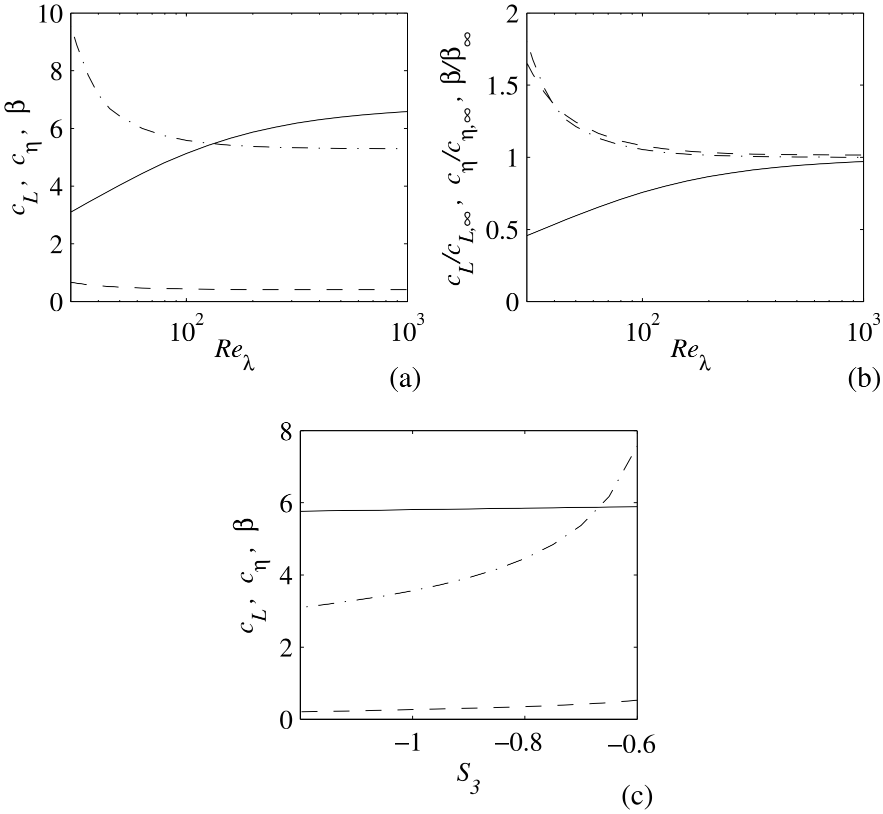

Figure 1. Variation of c_L (—), c_η (−−) and β (−·) with Re_λ and $\mathcal{S}_3$: (a) variation with Re_λ for $\mathcal{S}_3 = -0.7$; (b) same as (a), but normalized with asymptotic values at $Re_\lambda = \infty$, with $c_{L,\infty} = 6.783, c_{\eta,\infty} = 0.402$ and $\beta_\infty = 5.3$; (c) variation with $\mathcal{S}_3$ for $Re_\lambda = 200$.

the Reynolds number, once $Re_\lambda > 100$. In contrast, c_L evolves much slower to its asymptotic value. Dependence of c_L, c_η and β on $\mathcal{S}_3$ at constant Reynolds number is addressed in figure 1(c). From this, it is understood that c_L shows almost no dependence on $\mathcal{S}_3$. In contrast, β and—to a lesser extent—c_η are strongly dependent on the skewness of the longitudinal velocity derivative. Furthermore, $\beta(\mathcal{S}_3)$ displays a vertical asymptote at $-0.5 > \mathcal{S}_3 > -0.6$ of which the exact value depends slightly on the Reynolds number. For $\mathcal{S}_3 \geq -0.5$, (21) has no solution.

A plot of the damping function $F(kL)$ and the corresponding dimensionless energy spectrum $G(kL)$ is presented in figures 2(a) and (b) respectively for $Re_\lambda = 50$, 100 and 200. $G(kL)$ is defined as

$$G(kL) = (kL)^{-5/3}F(kL) = Re_L^{-5/4}g(k\eta). \tag{22}$$

It can be observed from the figure that the large scales start to be independent of the Reynolds number at increasing Reynolds numbers. Also, in both plots an inertial subrange can be observed, which elongates with increasing Reynolds numbers and, hence, accompanied by a shift of the dissipation range to higher wavenumbers.

2.3. Energy spectra for finite simulation domains

In practical LES applications, the simulation domain is finite. Hence, in (14)–(16), (20), (21), etc, the integration over continuous Fourier spectra should be replaced by a summation over a

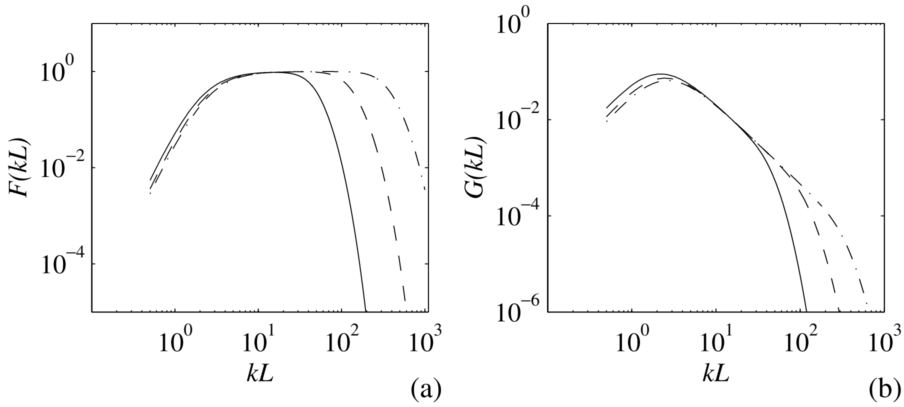

Figure 2. (a) Damping function $F(kL)$ and (b) dimensionless spectrum $G(kL)$ for $\mathcal{S}_3 = -0.7$ and $Re_\lambda = 50$ (—), $Re_\lambda = 100$ (−−) and $Re_\lambda = 200$ (−·).

discrete Fourier series. The elaboration towards the corresponding discrete consistency relations for finite domain systems is briefly summarized here.

Typically, LES and DNS of homogeneous isotropic turbulence is performed on a box with periodic boundary conditions. Consider $a = \mathcal{L}/L$, the ratio between the box size $\mathcal{L}$ and the integral length scale L. In this case, Fourier modes only exist at a discrete set of wavenumbers, i.e.

$$k = i\frac{2\pi}{\mathcal{L}} = i\frac{2\pi}{aL} \quad \text{with} \quad i \in \mathbb{N}. \tag{23}$$

The zeroth, second and fourth moments are now expressed as Fourier sums, and (14), (15) and (20) are replaced by

$$M_0 \equiv \left(\frac{2\pi}{aRe_L^{3/4}}\right)\sum_{i=0}^{\infty} g\left(i\frac{2\pi}{aRe_L^{3/4}}\right) = \frac{Re_L^{1/2}}{\alpha}, \tag{24}$$

$$M_2 \equiv \left(\frac{2\pi}{aRe_L^{3/4}}\right)^3\sum_{i=0}^{\infty} i^2 g\left(i\frac{2\pi}{aRe_L^{3/4}}\right) = \frac{1}{2\alpha} \tag{25}$$

and

$$M_4 \equiv \left(\frac{2\pi}{aRe_L^{3/4}}\right)^5\sum_{i=0}^{\infty} i^4 g\left(i\frac{2\pi}{aRe_L^{3/4}}\right) = \frac{-7\mathcal{S}_3}{12\sqrt{15}\alpha}. \tag{26}$$

Evidently, for $a \to \infty$, (24)–(26) converge to the continuous formulations in (14), (15) and (20). The sensitivity of c_L, c_η and β to variations of a is depicted in figure 3(a) at $Re_\lambda = 100$ and $\mathcal{S}_3 = -0.7$. It is readily seen that the continuous limit is already approached for $a > 4$. Furthermore, mainly c_L is strongly dependent on a, whereas c_η and β display a minimal variation for $1 < a < 2$ only. In figure 3(b), energy spectra are displayed for three different settings of a. It may be observed that for $a = 1$, the spectrum is concave in the low-wavenumber range of the spectrum. This rather non-physical behaviour results from a computational box which is too small compared with the length scale of the energy containing eddies and is accompanied

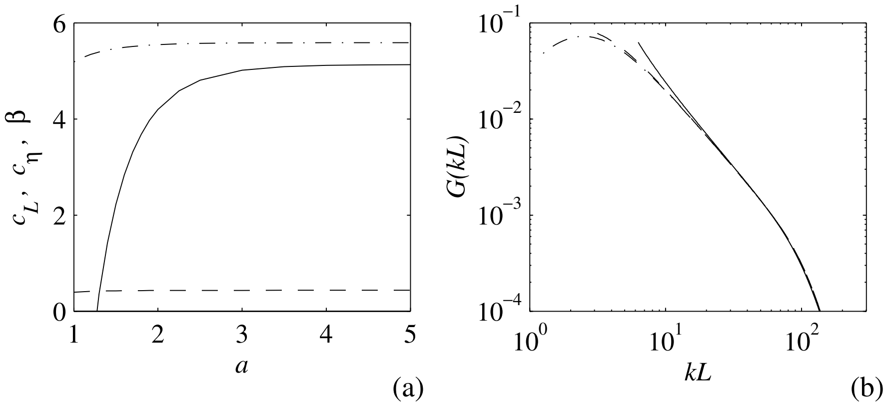

Figure 3. (a) Variation of c_L (—), c_η (−−) and β (−·) with a at $Re_\lambda = 100$ and $\mathcal{S}_3 = -0.7$. (b) Dimensionless spectra for $Re_\lambda = 100$ and $\mathcal{S}_3 = -0.7$, with $a = 1$ (—), $a = 2$ (−−) and $a = 5$ (−·).

with negative values for c_L. In brief, the results in figure 3 allow one to conclude that a valid representation for the energy spectrum can be obtained for $a \geq 2$, whereas for $a > 4$, the energy spectrum is independent of a.

3. Estimation of subgrid statistics

This section provides a thorough evaluation of subfilter energy in homogeneous isotropic turbulence, depending on Reynolds number, LES-filter width, etc. First, in section 3.1, the subfilter energy is evaluated based on the analytical descriptions of the energy spectra for homogeneous isotropic turbulence, which were discussed in detail in the previous section. Furthermore, a detailed evaluation of the subfilter energy as function of the Reynolds number Re_λ, and the ratios L/Δ and a is provided with specific attention to asymptotic behaviour. Next, in section 3.2, the prediction methodology is validated against evaluations of subfilter energy based on actual DNS at two different Reynolds numbers. Finally, some comments are provided in section 3.3 on the formulation of a subfilter-energy model, which can be effectively used during a large-eddy simulation.

3.1. *A priori* estimation of the subfilter energy

The subfilter or subgrid energy is defined as

$$E_{sgs} = \tfrac{1}{2}\langle u_i u_i - \overline{u}_i \overline{u}_i \rangle \tag{27}$$

with $\overline{(\cdot)}$ a sharp cut-off filter. It is evident that this property can be evaluated independent of the LES methodology, and only depends on the choice of the LES filter. In the present paper, we adopt a cut-off $k_\Delta = \pi/\Delta$. With use of the the semi-empirical energy spectra discussed in section 2, it is now possible to construct an *a priori*, simulation-independent tool with which E_{sgs} can be estimated. This methodology is elaborated and evaluated in the present subsection.

With use of the energy spectrum and the filter cut-off, the subgrid energy can be easily expressed as

$$E_{sgs} = \int_{k_\Delta}^{\infty} \alpha \varepsilon^{2/3} k^{-5/3} F(kL)\, \mathrm{d}k. \tag{28}$$

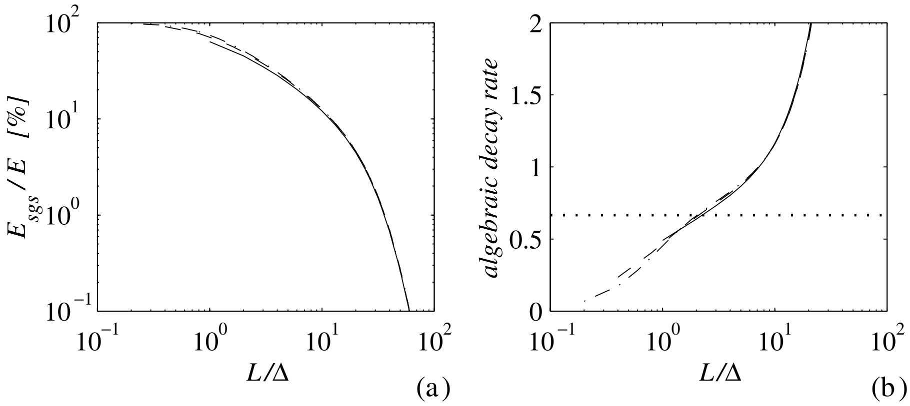

Figure 4. (a) Variation of the subfilter kinetic energy with L/Δ for $Re_\lambda = 100$ and different values of a. (b) Algebraic rate of decrease of the subfilter energy. (—): $a = 2$; (−−) $a = 5$; (−·) $a = 10$. (···), asymptotic rate of decrease for $Re_\lambda = \infty$.

Here, $F(kL)$ is a damping function conforming to the relevant consistency relations (cf section 2). From a dimensional analysis, it is readily understood that the ratio E_{sgs}/E, with E the total energy, depends on Re_λ, the ratio L/Δ, and, for the periodic case, the ratio $\mathcal{L}/L = a$. Equation (28) can be evaluated numerically for different settings of Re_λ, L/Δ and a. For the periodic case, this amounts to the execution of a summation, similar to (24) but for a different normalization, and a starting index corresponding to the cut-off wavenumber $k_\Delta = \pi/\Delta$. Since, for high values of k, the energy spectrum decreases exponentially with k, a simple convergence criterion, based on the relative subgrid energy increment, can be used.

Comparison of this methodology with the more simple $k^{-5/3}$ spectrum is straightforward and corresponds to the $Re_\lambda \to \infty$ limit, with $k_\Delta L \gg 1$. The choice of the simpler $-5/3$ spectrum allows for an analytical solution of the integration

$$E_{sgs} = \int_{k_\Delta}^{\infty} \alpha \varepsilon^{2/3} k^{-5/3}\, \mathrm{d}k. \tag{29}$$

In combination with (3), this leads to

$$\frac{E_{sgs}}{E} = \frac{3\alpha}{2\pi^{2/3}} \left(\frac{\Delta}{L}\right)^{2/3}. \tag{30}$$

This expression, which represents the asymptotic behaviour of (28), is—in similar forms—regularly encountered in the literature (see e.g. [8, 14]). Equation (30) suggests that, for high Reynolds numbers, the subgrid energy decreases algebraically with Δ to the power 2/3.

In figure 4, the subfilter energy is evaluated for a constant Reynolds number ($Re_\lambda = 100$) and different values of a. In figure 4(a), the subfilter energy is plotted versus the number of filter widths pro integral length scale L/Δ (which is, in practice, related to the LES resolution). Differences in energy for different values of a are small and only visible for very small values of L/Δ. Furthermore, in figure 4(b), the algebraic decay rate of the subfilter energy is plotted together with the 2/3 value, which corresponds to the use of a $-5/3$ spectrum and is valid for high Reynolds numbers. Here again, the curves are almost independent of a. Moreover, it can be observed that for $Re_\lambda = 100$, E_{sgs}/E decreases faster than algebraically with Δ/L.

From the sensitivity analysis of the energy spectra as function of a in section 2.2, one could already conclude that the shape of these spectra was relatively independent of a, when $a > 4$. In figure 4, this trend is clearly visible for the results corresponding to $a = 5$ and 10. Moreover,

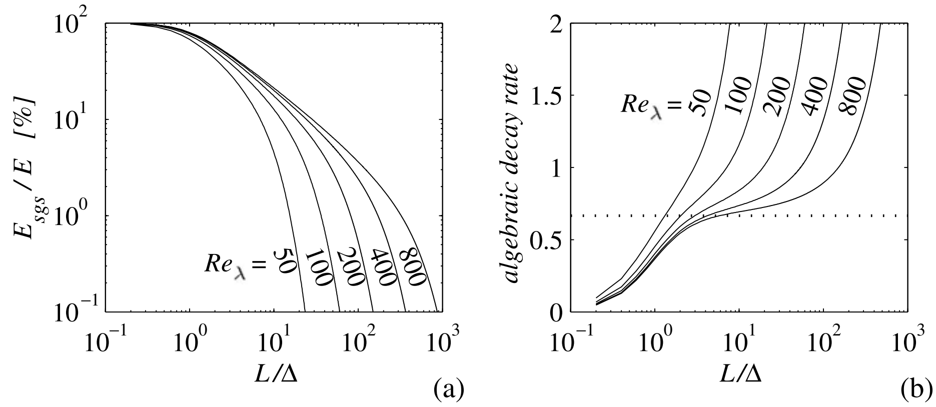

Figure 5. (a) Variation of the relative subfilter kinetic energy with L/Δ for $a = 10$ and different values of Re_λ. (b) Algebraic rate if convergence of the subfilter energy. $(\cdots)$, asymptotic rate of convergence for $Re_\lambda = \infty$.

for relative subgrid-energy levels $E_{sgs}/E < 10\%$, one can easily conclude that the presented curves are independent of a, even for low values such as $a = 2$. This illustrates that E_{sgs}/E at relevant levels (below 10%) is independent of the precise large-scale shape of the spectrum. At intermediate to high Reynolds numbers, it is generally accepted that the intermediate to small turbulent scales in free shear flows are homogeneous and isotropic. This, together with the previous observation on the independence of E_{sgs} on a, invites to presume that the present methodology to determine E_{sgs}, can be applied to free shear flows in general.

Figure 5 presents the subgrid energy for different values of the Reynolds number. Again, figure 5(a) displays the energy itself, whereas figure 5(b) shows its algebraic decay rate with filter width. Although expression (30) suggests Reynolds-independent subgrid energy at high Reynolds number, the relative error seems to be only independent for $E_{sgs}/E > 10\%$ and $Re_\lambda > 400$. An analysis of the asymptotic 2/3th power shows that for higher Taylor Reynolds numbers, the theoretical decay is more and more approximated for intermediate values of L/Δ. From this it is clear that the 2/3 decay strongly depends on the existence of an extensive inertial subrange. For higher values of L/Δ, one notices that the algebraic rate of decay starts to increase rapidly. This behaviour is connected to the dissipation range, where the energy decrease is exponential. For a subfilter-energy level of 1%, it can be observed that the exponent of decay is larger than 2 for $Re_\lambda < 400$, whereas for $Re_\lambda \geq 400$, the exponent is always lower than 2. These results clearly suggest that the use of a simplified $k^{-5/3}$ spectrum should be carefully limited to relatively high Reynolds-number cases. This is further illustrated in the next paragraph.

To summarize the effects of L/Δ and Re_λ on E_{sgs}/E and further investigate the range in which the simplified asymptotic $-5/3$ spectrum can be used, figure 6 displays two contours of constant subfilter energy, i.e. $E_{sgs}/E = 1$ and 5%, on a L/Δ versus Re_λ map. In this figure, the level of subfilter energy can be estimated for a choice of L/Δ and Re_λ. Consequently, the need for a subfilter-energy model can be assessed. One can see the $Re = \infty$ asymptotes for both $E_{sgs}/E = 1$ and 5%. In fact, these asymptotes correspond to (30). As can be appreciated for the two choices of relative subfilter energy, this asymptote is only approximated at relatively high Reynolds numbers, i.e. $Re_\lambda > 1000$.

A further study on the difference between a subgrid energy estimation according to (30) and an estimation following (28) can be performed. To this end, define

$$\delta_E^{sgs} = \frac{E^*_{sgs} - E_{sgs}}{E}, \tag{31}$$

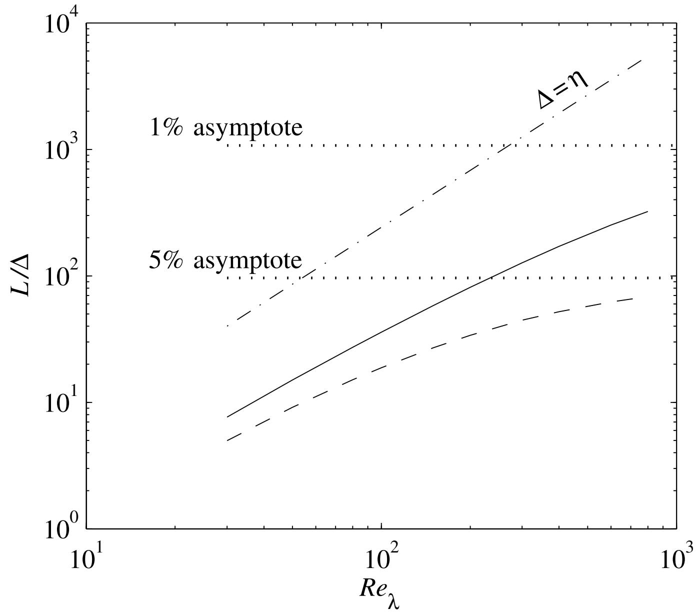

Figure 6. Required ratio of L/Δ as function of Re_λ (with $a = 2$) for different levels of subfilter energy, i.e. $E_{sgs}/E = 1\%$ (—) and $E_{sgs}/E = 5\%$ (−−), respectively. (−·) $\Delta = \eta$; (···) respective asymptotes according to (30).

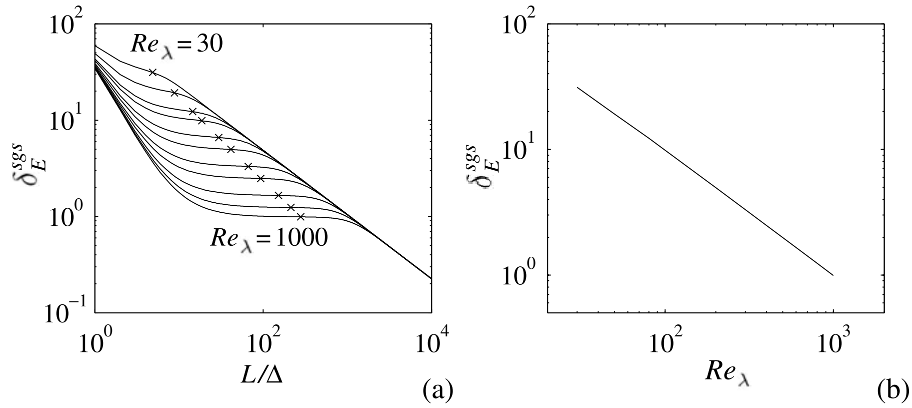

Figure 7. (a) Difference between (30) and (28) for the evaluation of the subgrid energy. (—) δ_E^{sgs} for $Re_\lambda = 30, 50, 80, 100, 150, 200, 300, 400, 600, 800$ and 1000; (×) inflection points. (b) δ_E^{sgs} of the inflection points as function of Re_λ.

where E^*_{sgs} follows from (30), i.e. based on the use of a simplified energy spectrum, and E_{sgs} is obtained from (28). Note that the relative difference is normalized using the total energy E.

In figure 7(a), δ_E^{sgs} is displayed for different Reynolds numbers as a function of L/Δ. For very high values of L/Δ, one can observe that δ_E^{sgs} decays as $(L/\Delta)^{-2/3}$. This is evident, since E^*_{sgs} (cf equation (30)) decays with the same power, whereas E_{sgs} (cf (28) and section 2) decays exponentially with (L/Δ). For low values of L/Δ, δ_E^{sgs} increases rapidly with decreasing L/Δ. This clearly results from the shape of the low-wavenumber spectrum, which differs significantly from $k^{-5/3}$. In between these extremes, most pronounced for higher values of the Taylor Reynolds

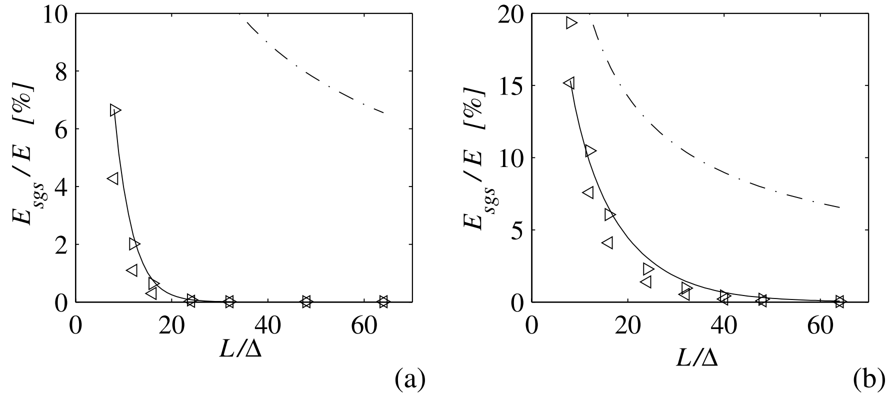

Figure 8. Subfilter energy for (a) $Re_\lambda = 50$ and (b) $Re_\lambda = 100$, and $a = 2$. (—) *a priori* prediction (equation (28)); ($-\cdot$) prediction based on an idealized $-5/3$ spectrum (equation (30)); ($\triangleright$) energy obtained from DNS with a spherical sharp cut-off filter; ($\triangleleft$) energy obtained from DNS with a cubic sharp cut-off filter.

number, δ_E^{sgs} displays a plateau. This region typically corresponds to a selection of the cut-off filter in the inertial subrange. To determine the level of this plateau as a function of Reynolds number, the inflection of the curves are determined. In figure 7(b), δ_E^{sgs} at these inflection points is plotted against Re_λ. As can be appreciated from this figure, the difference between both evaluations of the subgrid energy approximately decreases with Re_λ^{-1}.

3.2. *A posteriori* evaluation of the subfilter energy on DNS data

To assess the quality of the prediction methodology presented in the previous subsection, the predicted subgrid energy is compared with the subgrid energy obtained from sharp cut-off filtering of DNS results. To this end, two DNS of decaying homogeneous isotropic turbulence are performed at $Re_\lambda = 50$ and 100. A detailed discussion on the DNS set-up and results, including a thorough convergence study, is presented in [23].

Both DNS are filtered with two types of sharp cut-off filters: the first, a spherical sharp cut-off, corresponding to the formalism in the previous section; and the latter, a cubic sharp cut-off filter, often encountered in practical simulations. For the spherical realization of the sharp cut-off filter, all modes outside a sphere with radius π/Δ (in spectral space) are removed; for the cubic realization, all modes outside a cube with size π/Δ are eliminated. To obtain one single value for the subgrid energy, an integration of the subgrid energy over the simulation time interval and a normalization corresponding to

$$\left(\frac{E_{sgs}}{E}\right)_{DNS} = \left(\frac{\int E^2_{sgs,\,DNS}\,\mathrm{d}t}{\int E^2_{DNS}\,\mathrm{d}t}\right)^{1/2} \tag{32}$$

are performed.

In figure 8, the subfilter energy is displayed for both Reynolds numbers. In this figure, the energy obtained from DNS, with use of a spherical and cubic sharp cut-off filter as well as the results of the *a priori* prediction (equation (28)) are displayed. As a point of reference, the prediction using an idealized $k^{-5/3}$ spectrum (equation (30)) is also displayed.

It is readily observed that both realizations of the sharp cut-off filter provide slightly different results for E_{sgs}/E, but correspond well with the *a priori* prediction (equation (28)). However, as might be expected, the results of the prediction methodology correspond closer to the spherical sharp cut-off filtered DNS. The DNS results are obtained from *decaying* homogeneous isotropic turbulence, with an *initial* Taylor Reynolds number of 100 and 50. During the decay, the energy will decrease, whereas the Taylor length scale is roughly constant, such that the Taylor Reynolds number also decreases. Hence, the mean Taylor Reynolds numbers of the DNS are lower than 100 and 50. This explains the differences between the *a priori* prediction and the spherical cut-off filtered DNS. Nevertheless, agreement is quite well over the full L/Δ range. In contrast, as is clear in figure 8, the use of a $k^{-5/3}$ spectrum (equation (30)) provides too large values for the subgrid energy.

3.3. A subfilter-energy model for direct use in LES

Again, the effective subfilter-energy model is based on the analytical descriptions of the energy spectra for homogeneous isotropic turbulence, which were discussed in detail in section 2. To fix these semi-empirical functions, during an LES run, one needs to know three different properties. In section 2, the total energy level E, the integral length scale L and the Reynolds number Re_λ were proposed. However, in an actual LES, the Reynolds number and the integral length scale L (according to its definition in (3)) are not easily accessible. Furthermore, only the resolved energy E_{res} is known. In fact, the effective aim of a subfilter-energy model for direct use in LES, is to determine the subfilter energy E_{sgs}, and hence, the total energy $E = E_{res} + E_{sgs}$. Therefore, the formulation presented in section 2 is slightly adapted.

During LES, one has access to the viscosity ν, to the total dissipation

$$\varepsilon = \langle 2\nu S_{ij} S_{ij} \rangle - \langle \tau_{ij}^M S_{ij} \rangle, \tag{33}$$

and further to the resolved energy

$$E_{res} = \tfrac{1}{2} \langle \overline{u}_i \overline{u}_i \rangle \, . \tag{34}$$

Here S_{ij} is the strain tensor and τ_{ij}^M is the model for the subgrid stresses $\tau_{ij} = \overline{u_i u_j} - \overline{u}_i \overline{u}_j$.

Based on ε and ν, the Kolmogorov scale can be calculated, i.e. $\eta = (\nu^3/\varepsilon)^{1/4}$. The integral length scale L cannot directly be determined. Therefore, the dimensionless forms f_L and f_η are formulated slightly different and combined into

$$f(k) = \left(\frac{k}{[k^2 + k_L^2]^{1/2}} \right)^{11/3} \exp(-\beta\eta([k^4 + k_\eta^4]^{1/4} - k_\eta)), \tag{35}$$

with $k_L = \sqrt{c_L}/L$ and $k_\eta = c_\eta/\eta$. Now, a set of relations can be formulated to determine k_L, k_η and β. First of all, it is possible to express the resolved energy as

$$E_{res} = \int_0^{\pi/\Delta} \alpha \varepsilon^{2/3} k^{-5/3} f(k) \, \mathrm{d}k, \tag{36}$$

with an integration limit determined by the filter width. The total dissipation ε can be expressed as

$$\varepsilon = 2\nu \int_0^\infty \alpha \varepsilon^{2/3} k^{1/3} f(k) \, \mathrm{d}k. \tag{37}$$

To ensure an economic solution algorithm, one can decide to keep β constant, e.g. a value of 5.3 might be used (cf figure 1). Alternatively, an additional equation—equivalent to (20)—has to be solved, i.e.

$$\int_0^\infty \alpha \varepsilon^{2/3} k^{7/3} f(k) \, \mathrm{d}k = \frac{-7\mathcal{S}_3 \varepsilon^{2/3}}{12\sqrt{15}\eta^{10/3}}. \tag{38}$$

Once k_L, k_η and β are solved, one can evidently determine the subgrid energy by integrating the unresolved part of the spectrum. The formulation of (36)–(38) for finite simulation domains—similar to the procedure in section 2.3—is straightforward.

Clearly, this model is constructed for equilibrium turbulence. Only effective testing can indicate how strictly this condition should apply. Furthermore, the large-scale formulation of the used spectra is mainly valid for homogeneous isotropic turbulence. Several arguments have been presented above, which suggest that the model might be applicable in shear flows. However, in this case, ensemble averaging, e.g. needed in (33), cannot be performed over three periodic directions and the corresponding use of three-dimensional energy spectra is—especially at low wavenumbers—artificial. To solve this, similar procedures to those in the present paper, based on one-dimensional formulations of energy spectra in space, or even time, might be envisaged.

4. Conclusions

Based on the use of semi-empirical functions for energy spectra of homogeneous isotropic turbulence [13], a methodology is presented for the determination of subgrid energy in large-eddy simulations. This formalism can be used for an *a priori* estimation of the subfilter energy, e.g. as part of a preparatory LES study, but can also be adapted for use in actual LES calculations as part of a subgrid-scale model.

In the literature, several examples are known which use a simplified $k^{-5/3}$ spectrum for the estimation of subgrid energy, stresses, etc [8, 12]. The use of more sophisticated spectra allows for the inclusion of several relevant physical parameters such as the Reynolds number and the integral length scale and its ratio to the flow containment. A comprehensive sensitivity analysis is presented. Furthermore, charts are drawn which are of direct use for an *a priori* estimation of subgrid-energy level depending on Reynolds number and selected LES resolution. In addition, the differences between a simplified $-5/3$ spectrum and the more sophisticated formulations are quantified. As can be expected, the results of the $-5/3$ assumption constitute the asymptotic high-Reynolds-number behaviour for the latter formulation. However this asymptotic behaviour is only approximated for $Re_\lambda > 1000$.

Results of the subfilter-energy model are validated based on the evaluation of DNS of decaying homogeneous isotropic turbulence. Agreement between *a priori* prediction and effective measured subfilter energy in filtered DNS is satisfactory. Finally, the formalism to estimate the subfilter energy is slightly adapted such that it can effectively be used during a large-eddy simulation as part of a subgrid-scale model.

Acknowledgments

This research was performed in the framework of FWO-project G.0130.02. We express our gratitude for the financial support by FWO-Vlaanderen.

References

[1] Geurts B J 2003 *Elements of Direct and Large-Eddy Simulation* (Flourtown, PA: Edwards)

[2] Lesieur M and Métais O 1996 New trends in large-eddy simulations of turbulence *Ann. Rev. Fluid Mech.* **28** 45–82

[3] Mason P J 1994 Large-eddy simulation: a critical review of the technique *Q. J. R. Meteorol. Soc.* **120** 1–26

[4] Rogallo R S and Moin R 1984 Numerical simulations of turbulent flows *Ann. Rev. Fluid Mech.* **16** 99–137

[5] Sagaut P 2002 *Large Eddy Simulations for Incompressible Flows* 2nd edn (Berlin: Springer)

[6] Geurts B J and Leonard A 2002 Is LES ready for complex flows? *Closure Stategies for Turbulent and Transitional Flows* ed B Launder and N Sandham (Cambridge: Cambridge University Press)

[7] Ghosal S, Lund T S, Moin P and Akselvoll K A 1995 A dynamic localization model for large-eddy simulation of turbulent flows *J. Fluid Mech.* **286** 229–55

[8] Misra A and Pullin D I 1997 A vortex-based subgrid stress model for large-eddy simulation *Phys. Fluids* **9** 2443–54

[9] Schumann U 1975 Subgrid scale model for finite difference simulations of turbulent flows in plane channels and annuli *J. Comput. Phys.* **18** 376–404

[10] Speziale C G 1991 Analytical methods for the development of Reynolds-stress closures in turbulence *Ann. Rev. Fluid Mech.* **23** 107–57

[11] Comte-Bellot G and Corrsin S 1971 Simple eulerian time corralation of full- and narrow-band velocity signals in grid-generated, 'isotropic' turbulence *J. Fluid Mech.* **48** 273–337

[12] Knaepen B, Debliquy O and Carati D 2002 Subgrid-scale energy and pseudo pressure in large-eddy simulation *Phys. Fluids* **14** 4235–41

[13] Pope S B 2000 *Turbulent Flows* (Cambridge: Cambridge University Press)

[14] Jiménez J and Moser R D 2000 Large-eddy simulations: where are we and what can we expect? *AIAA J.* **38** 605–12

[15] Lilly D K 1967 The representation of small-scale turbulence in numerical simulation experiments *Proc. IBM Scientific Computing Symp. on Environmental Sciences* IBM Data Processing Division, White Plains, New York

[16] Lumley J L 1967 Similarity and the turbulent energy spectrum *Phys. Fluids* **10** 855–8

[17] Monin A S and Yaglom A M 1975 *Statistical Fluid Mechanics II: Mechanics of Turbulence* (New York: MIT Press)

[18] Hinze J O 1975 *Turbulence McGraw-Hill Series in Mechanical Engineering* 2nd edn (New York: McGraw-Hill)

[19] Kolmogorov A N 1991 Dissipation of energy under locally isotropic turbulence *Proc. R. Soc.* A **434** (first published in 1941 *Dokl. Akad. Nauk SSSR* **32** 16–8)

[20] Kolmogorov A N 1991 The local structure of turbulence in an incompressible fluid for very large Reynolds numbers *Proc. R. Soc.* A **434** (first published in 1941 *Dokl. Akad. Nauk SSSR* **30** 301–5)

[21] Kolmogorov A N 1991 On the degeneration of isotropic turbulence in an incompressible viscous fluid *Proc. R. Soc. Ser.* A **434** (first published in 1941 *Dokl. Akad. Nauk SSSR* **31** 538–40)

[22] Batchelor G K 1953 *The Theory of Homogeneous Turbulence. Cambridge Monographs on Mechanics and Applied Mathematics* (Cambridge: Cambridge University Press)

[23] Meyers J, Geurts B J and Baelmans M 2003 Database-analysis of errors in large-eddy simulation *Phys. Fluids* **15** 2740–55